Aerodynamic behavior of an airfoil under extreme wind conditions

Ingrid Neunaber, Caroline Braud

Aerodynamic behavior of an airfoil under extreme wind conditions

Ingrid Neunaber
&
Caroline Braud

Motivation

- wind in the atmosphere is turbulent ⇒ turbulence increases loads [1]
- wind turbine savety and durability guaranteed by design requirements from IEC-61400-1 norm: extreme wind conditions are accounted for [2]
- interaction between complex, rapid flow structures and the rotor blade is not well understood: aerodynamic behavior of an airfoil is highly dependent on dynamic variations of the angle of attack between the flow and the blade

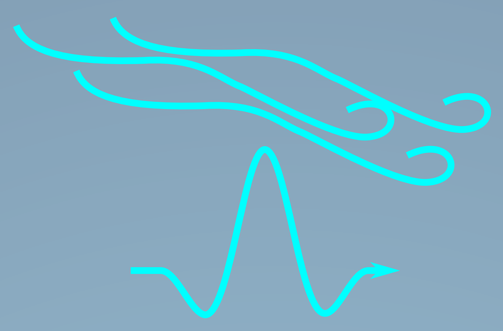

Extreme operating conditions are modeled with a Mexican hat wave-let in [1]. A typical gust factor $G_I = \frac{U_{max}}{U_I}$ of $G_{I,IEC}$ = 1.27 is reached at an inflow velocity u_0= 20 ms^{-1} [5]. U_{max} is the maximum wind speed in a time interval ΔT and U_I the mean wind speed in ΔT.

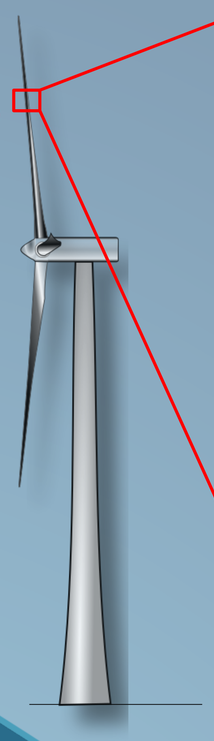

A

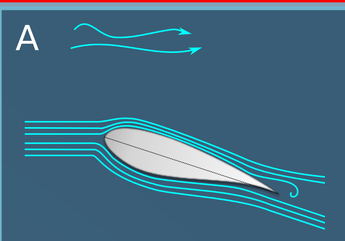

A: regular inflow
The **flow is attached** to the airfoil and the wind turbine operates normally. The control can account for changes in the inflow.

B

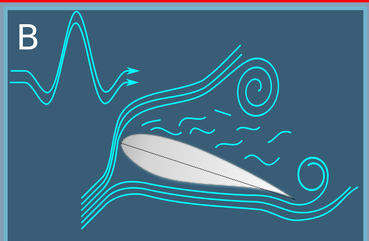

B: gust
A sudden change in the inflow velocity, i. e. a **gust**, causes a sudden change in the angle of attack at the rotor blade which leads to an overshoot in lift due to **dynamic stall** and results in **high loads**. Control mechanisms do not operate fast enough to avoid this.

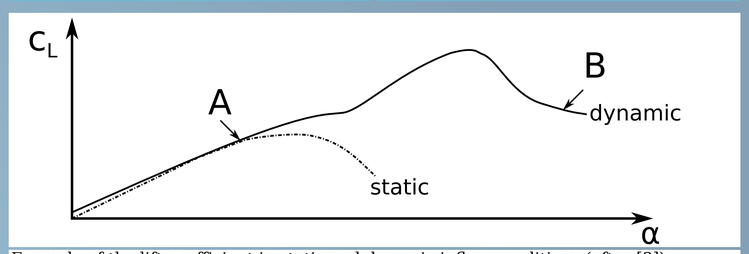

Example of the lift coefficient in static and dynamic inflow conditions (after [3]).

Objectives

- introduce a **setup** capable of producing strong, rapid flow variations while also including **turbulence**
- **characterize** the **flow** generated by this setup
- **expose an airfoil** to the inflow and investigate the impact of extreme flow variations on the lift response of the airfoil

Setup

The Chopper
Strong, rapid flow perturbations are generated by a rotating bar that cuts through the inlet of the wind tunnel [4]. Turbulence is added by a regular grid

Look at the video here!

A. Front view

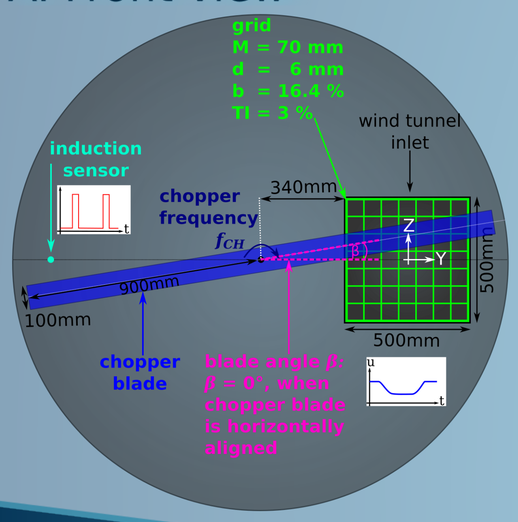

B. Setup

Airfoil exposed to inv. gust

- 3 airfoil angles:
  α_{01} = 0°
  α_{02} = 8°
  α_{03} = 12°
- 2 chopper frequencies:
  f_{CH1} = 0.04 Hz (t = 600 s)
  f_{CH2} = 0.4 Hz (t = 120 s)
- inflow measured with cobra probe at f_S = 2.5 kHz
- inflow velocity u_0 = 18 ms^{-1}

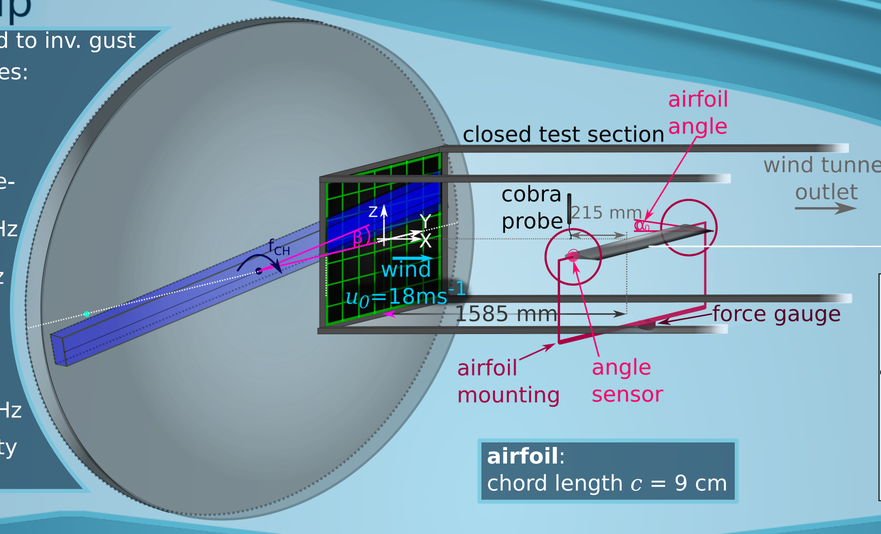

airfoil:
chord length c = 9 cm

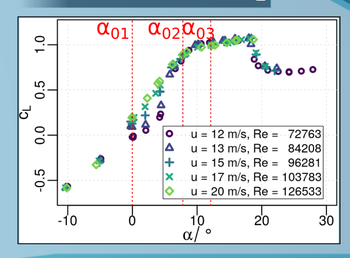

Results: Inflow

The inverse Gust
- large, rapid velocity deficit in U induced by chopper:
  ΔU_1 = 5.2 ms^{-1} / ΔU_2= 6.2 ms^{-1}
- shape of inverse gust depends on chopper frequency
- variations in v and w component
- gust duration Δt ~ anti-proportional to chopper frequency:
  $\Delta t \approx$ 7.3s(f_{CH1}) / $\Delta t \approx$ 0.8s(f_{CH2})
- TI≈17% (f_{CH1}) / TI≈13% (f_{CH2})
- G_I≈1.16 (f_{CH1}) / G_I≈1.2 (f_{CH2})

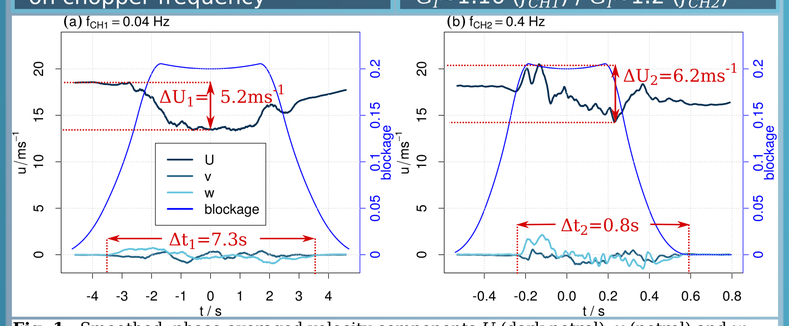

Fig. 1: Smoothed, phase-averaged velocity components U (dark petrol), v (petrol) and w (light petrol) for f_{CH1} = 0.04 Hz, (a), and f_{CH2} = 0.4 Hz, (b), and blockage (blue).

The energy spectral density
- hot-wire measurement with f_s= 50 kHz for high resolution
- periodic gust events in time series visible as peaks with f_{CH}
- turbulence in the gust decays [4]

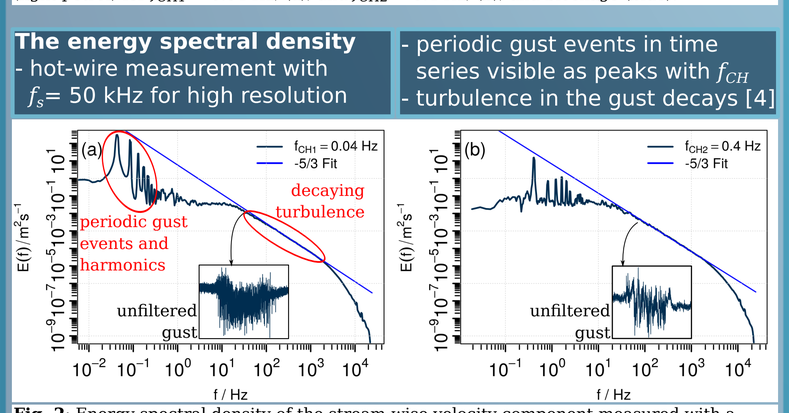

Fig. 2: Energy spectral density of the stream-wise velocity component measured with a hot-wire 21.5 cm in front of the airfoil (α_{02} = 7.8°) for the two chopper frequencies f_{CH1} = 0.04 Hz, (a), and f_{CH2} = 0.4 Hz, (b).

The mean flow field
- flow field in complete test section scanned with cobra probes
- fig.3:interpolated contour plot of normalized mean gust velocity
- flow inhomogeneous close to the inlet but more homogeneous downstream at airfoil position

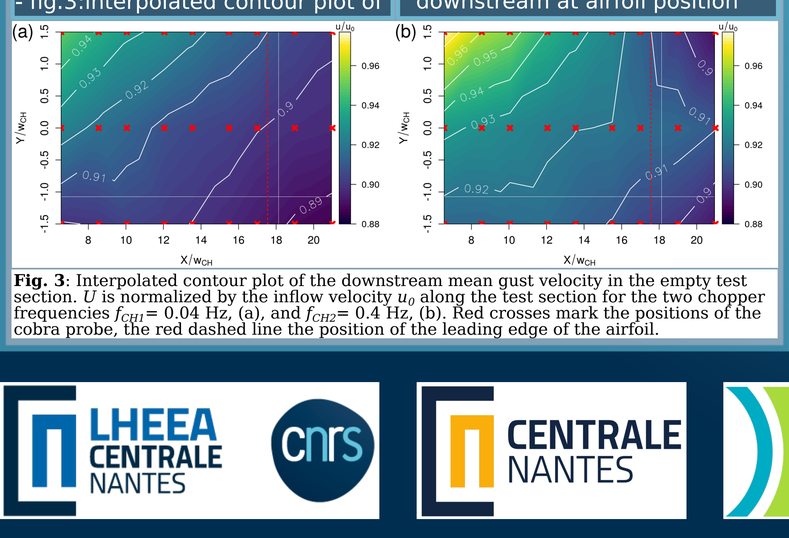

Fig. 3: Interpolated contour plot of the downstream mean gust velocity in the empty test section. U is normalized by the inflow velocity u_0 along the test section for the two chopper frequencies f_{CH1}= 0.04 Hz, (a), and f_{CH2}= 0.4 Hz, (b). Red crosses mark the positions of the cobra probe, the red dashed line the position of the leading edge of the airfoil.

Results: Airfoil

The airfoil response
- fig. 4 shows the response of the phase-averaged, smoothed lift force F_L to the gust for the three airfoil angles, the inflow velocity and the flow pitch angle ψ
  ⇒ **angle of attack: $\alpha = \alpha_0 + \psi$**
- the higher α_0, the higher F_L
- lift response follows mean flow component U of the inverse gust for both chopper frequencies
- small influence of ψ on F_L

The airfoil response: numbers

	α_0 / °	f_{CH1}	f_{CH2}
ΔU / ms^{-1}		5.2	6.2
$\Delta\psi$ / °		5.6	10.7
ΔF_L / N	-0.02	1.23	4.38
	7.8	4.33	5.32
	12.11	4.26	4.38

- for f_{CH1}, ΔF_L is significantly smaller for α_{01} than for α_{02} and α_{03}
- for f_{CH2}, ΔF_L is similar for all airfoil angles but largest for α_{02}

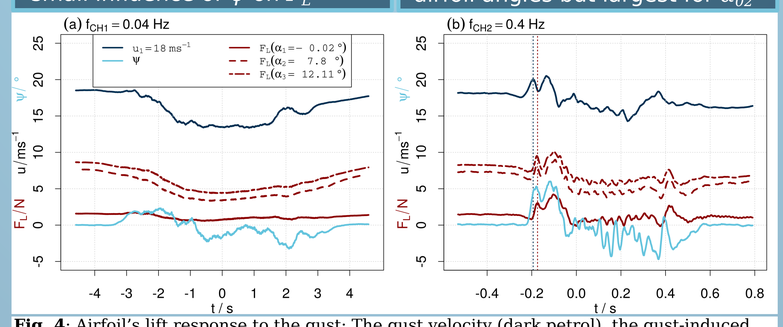

Fig. 4: Airfoil's lift response to the gust: The gust velocity (dark petrol), the gust-induced flow pitch angle ψ (light petrol) and the lift force response for the three airfoil angles −0.02°, 7.8° and 12.11° (red, different line types) are plotted for f_{CH1} = 0.04 Hz, (a), and f_{CH2} = 0.4 Hz, (b).

Simulated airfoil response
further investigation of the influence of U and ψ on the lift response of the airfoil
- interpolated surface fit of $c_L(\alpha, u_0)$ (cf. setup) used to calculace *expected* response of c_L to gust
- figure 5: influence of U and ψ can be separated by calculating c_L with respect to U (- -), ψ (···), and both U and ψ (—) for α_{02}
- additionally: measured c_L(—)

Main results
- the simulated $c_L$response is determined by change of α
- with respect to only U, c_L would be constant
- the simulated and measured c_L are in the same order of magnitude but differ significantly in case of f_{CH1} ⇒ dynamic aerodynamic effects present
- for the rapidly changing flow of f_{CH2}, α does determine evolution

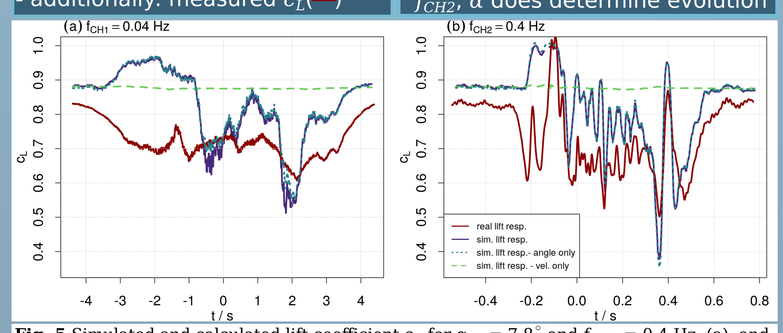

Fig. 5:Simulated and calculated lift coefficient c_L for α_{02} = 7.8° and f_{CH1} = 0.4 Hz, (a), and f_{CH2} = 0.04 Hz, (b), respectively: c_L is simulated with respect to the gust velocity and gust-induced flow pitch angle (purple), the gust-induced flow pitch angle only (turquois, dotted), and the velocity only (green, dashed).

Conclusions

- **new setup** for generation of complex, strong, turbulent flow changes for aerodynamic investigations presented: the *chopper*
- 2 different chopper frequencies investigated
- main **flow features** include
  - rapid strong inverse gust
  - decaying turbulence within gust (cf. [4])
  - changes of the mean velocity of over 5 ms^{-1} in less than 2s (f_{CH1}) / 0.4s (f_{CH2})
  - variation of v and w flow component during gust ⇒ dynamic angle of attack changes investigatable!
- the **response of the airfoil** to the gust
  - appears to be mainly determined by mean velocity
  - a comparison with the simulated gust response shows that dynamic effects that cannot be explained by the static lift curve are present
- in the **future**, we plan to
  - further customize the setup to also generate increasing gusts
  - investigate the dynamic effects using non-instrusive flow measurements (PIV) and local aerodynamic characterization

Sources

[1] Frandsen S (2007) Turbulence and turbulence generated structural loading in wind turbine clusters, Phd thesis, *DTU - Risø National Laboratory*

[2] IEC 61400-1-4 (2019) Wind energy generation systems - Part 1: Design requirements, Report, *International Electrotechnical Commission*

[3] Choudhry A, Leknys R, Arjomandi M and Kelso R (2014) An insight into the dynamic stall lift characteristics, *Experimental Thermal and Fluid Science* **58**

[4] Neunaber I, Braud C (2020) First characterization of a new perturbation system for gust generation: The Chopper, *Wind Energy Science*, **5**

[5] Bardal L M and Sætran L R (2016) Wind gust factors in a coastal wind climate, *Energy Procedia* **94** 417–424

[6] Soulier A, Braud C, Voison D and Podvin B (2020) Ability of the e-TellTale sensor to detect flow features over wind turbine blades:flow stall/reattachment dynamics, *Wind Energy Science*,in review

Acknowledgements

This work was carried out within the research projects ASAPe with the funding from region Pays-de-Loire, Centrale Nantes, and Ville de Nantes (grant no. 2018 ASAPe) and ePARADISE with the funding from ADEME/region Pays-de-Loire (grant no. 1905C0030). The authors would like to thank WEAMEC. The authors would like to thank CSTB for providingmeasurement equipment.